Strain-amplified structural modulation of Bi-cuprate high-T_c superconductors

Satoru Kaneko and Kensuke Akiyama
Kanagawa Industrial Technology Research Institute, Kanagawa Prefectural Government, 705-1 Shimo-Imaizumi, Ebina, Kanagawa 243-0435, Japan

Hiroshi Funakubo
Department of Innovative and Engineered Materials, Tokyo Institute of Technology, 4259 Nagatsuta-cho, Midori-ku, Yokohama, Kanagawa 226-8502, Japan

Mamoru Yoshimoto
Materials & Structures Laboratory, Tokyo Institute of Technology, 4259 Nagatsuta-cho, Midori-ku, Yokohama, Kanagawa 226-8503, Japan

(Received 18 October 2005; revised manuscript received 29 June 2006; published 7 August 2006)

Two dimensional x-ray images of a multilayered bismuth high-temperature superconductor (HTS) together with reciprocal-space simulation have shown how unit cells are distorted to form "supercells," the structural modulation consisting of multiple unit cells with incommensurate modulation period in a HTS. Strain induced by the multilayered structure alters the lattice mismatch between bismuth and perovskite blocks, resulting in increased supercell distortion described by the amplitude in the modulation wave. While oxygen content affects the modulation period of the supercell, lattice mismatch dominates the displacement of each atom from its position in the perfect crystal to construct the distorted structure, the supercell.

DOI: 10.1103/PhysRevB.74.054503 PACS number(s): 74.62.Fj, 74.72.Hs

The bismuth cuprate high-T_c superconductor (HTS) includes both local geometry and global geometry in its crystal structure. Each unit cell of the local geometry is not evenly distributed in the global geometry. Rather, unit cells are incommensurately modulated in a large-scale structure, a *supercell*, which is a structural modulation consisting of multiple unit cells with incommensurate modulation period.[1–4] The supercell SC of $Bi_2Sr_2Ca_1Cu_2O_x$ (Bi-2212) can be expressed as $4.7b+1.0c$ on a single crystal, where b and c are the lattice constants along b and c axes, respectively. The SC structure has an incommensurate period along the b axis. Previous works have studied the modulation period, which specifies the size of the supercell. In addition to the modulation period, by using x-ray reciprocal space mapping (XRSM) we also estimated the modulation amplitude, which indicates how strongly unit cells are distorted to form the supercell, and showed that the oxygen content affects the modulation period while the lattice mismatch affects the modulation amplitude. These results indicate charge transfer in the multilayer structure.

Enormous efforts have been made in exploring the origin of the supercell employing largely one of two styles, oxygen doping and aliovalent substitution. Oxygen doping changes the oxygen content by annealing or by high-pressure oxidization. The aliovalent substitution of cations changes oxygen content by replacing divalent strontium with trivalent lanthanum, for instance. Both styles aim to intercalate extra oxygen into the supercell structure. Extra oxygen was once considered to be the origin of the supercell; however, the extra oxygen model does not explain the effect of the supercell on substitution for homovalent cations[5] or the substitution of $3d$ metals.[6] Putting aside the extra oxygen model, intrinsic strain induced by lattice mismatch between the bismuth and the perovskite block is a possible candidate for the origin of the supercell. When using aliovalent substitution, the differing radius of the substituting cations may cause strain in the crystal as well as the intercalation of extra oxygen.

Emphasizing the effect of intrinsic strain, we are proposing another method which is encompassed by neither oxygen doping nor aliovalent substitution: multilayer strain. External strain induced by bilayers in the multilayer must affect, the intrinsic strain between BiO and the perovskite block and would give rise to more prominent effects than aliovalent substitution on the supercell. X-ray diffraction (XRD) is a good method for observing the supercell structure (SC structure). Electron diffraction can observe only the $a\times b$ plane since the bismuth cuprate HTS grows c-axis orientated. Unlike electron diffraction, XRD observes the $b\times c$ plane on which the supercell structure spreads. We employed x-ray reciprocal space mapping to observe satellite peaks generated by the SC structure (SC peaks) in multilayered $Bi_2Sr_2Ca_1Cu_2O_x/Bi_2Sr_2Cu_1O_x$ (Bi-2201). XRSM of the multilayered structure indicated that the modulation amplitude

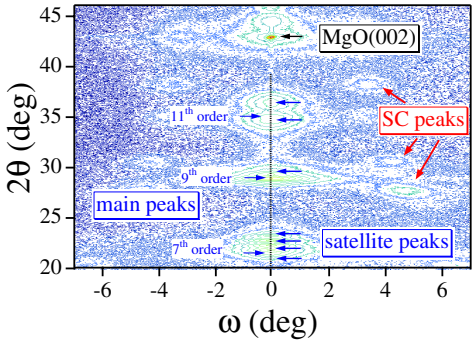

FIG. 1. (Color online) Wide-area cross section XRSM shows main peaks and MgO peak, together with satellite peaks generated by a multilayer period along the θ-2θ scan direction. Other satellite peaks generated by the SC structure are also observed around the main peaks.

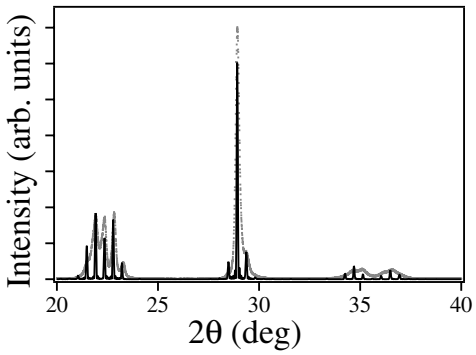

FIG. 2. θ-2θ scan extracted along the dashed line of the wide-area XRSM. The dots and solid lines are experimental and simulation spectra, respectively.

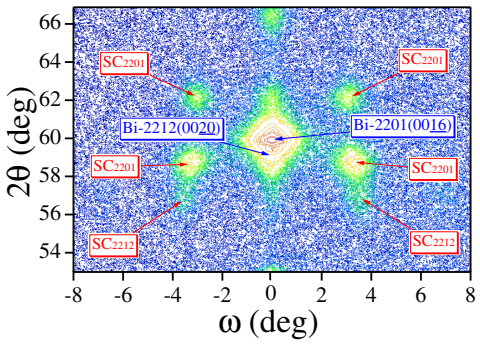

FIG. 3. (Color online) XRSM taken on $b\times c$ plane shows main peaks and SC peaks at a higher-angle region. The main peaks are no longer based on the multilayer period, rather the peaks are from separate Bi-2212 and Bi-2201 films. SC_{2201} shows symmetric SC peaks originating from Bi-2201(0016), while SC_{2212} shows asymmetric intensity distribution around Bi-2212(0020).

increased with multilayer strain and that modulation periods slightly expanded along the c axis.

Single- and multilayered samples were prepared by pulsed laser deposition using a slower Q-switched neodymium-doped yttrium aluminum garnet (Nd:YAG laser).[7] Using stoichiometric targets of Bi-2212 and Bi-2201, HTS films were deposited on MgO(100) substrates at a temperature of 750 °C, with a substrate-target distance of 40 mm. Epitaxial growth was verified by x-ray θ-2θ and ϕ scan, and multilayered structure was examined by simulation using a θ-2θ scan together with x-ray reflection. XRSM was performed on a cross section ($b\times c$ plane) and plan view ($a\times b$ plane) to observe SC peaks generated by the SC structure. Each single layer of Bi-2212 and Bi-2201 on a MgO(100) substrate showed lattice constants b of 5.43 and 5.39 Å, respectively. The lattice mismatch is about 0.7% between Bi-2212 and Bi-2201 layers. Resistivity measurements showed a depression of the transition temperature (R=0); single Bi-2212 and multilayered $(\text{Bi-2212}_4/\text{Bi-2201}_3)_6$ and $(\text{Bi-2212}_2/\text{Bi-2201}_2)_6$ had 70, 60, and 32 K as transition temperatures.

Figure 1 shows a wide-area cross section XRSM on a Bi-2212/Bi-2201 multilayered structure. Main peaks were observed at the average lattice constant of each layer in the multilayer (seventh, nineth and 11th order), together with satellite peaks generated by the thickness of the bilayer (multilayer period). Other satellite peaks generated by the SC structure were also observed around the main peaks. However, these SC peaks are not based on each layer of either Bi-2212 or Bi-2201, rather based on an artificial unit cell consisting of the multilayer period. Figure 2 shows such a main peak with its satellite peaks, extracted along the θ-2θ direction (dashed line). The x-ray reflectivity spectrum, taken together with satellite peaks on the θ-2θ scan, was indicative of chemical modulation maintained in the multilayered samples. Since the bismuth cuprate HTS has a layered structure consisting of alternating perovskite and BiO layers, diffraction peaks originate from the superimposing structure factor on each layer. A simulation using a one-dimension kinematic diffraction model can determine each lattice constant and multilayer period.[8–10] The solid line in Fig. 2 is a simulation pattern, which shows the multilayered structure to be $(\text{Bi-2212}_4/\text{Bi-2201}_3)_6$. With decreasing multilayer period, lattice constants in the multilayer became an average of two layers (5.41 Å) along the b axis, while the Bi-2212 layer extended to 31.09 Å along the c axis and contracted to 5.41 Å along the b axis. Bi-2201 contracted to 24.46 Å along the c axis and expanded to 5.41 Å along the b axis.

In the high-angle region, the main peaks are no longer dominated by the multilayer period; rather the main peaks become more like separate Bi-2212 and Bi-2201 peaks. Figure 3 shows the XRSM at a higher index on the multilayer. The XRSM shows both Bi-2201(0016) and Bi-2212(0020) peaks together with SC satellite peaks. Interestingly, only four layers of the Bi-2212 film raised SC satellite peaks around the main peak of Bi-2212(0020). As with previous reports,[10–12] Bi-2201 showed four SC peaks around the main peak and Bi-2212 shows asymmetric distribution of SC

TABLE I. A summary of the parameters on Bi-2212 shows lattice constants (Å) and modulation periods (Å) SC_b and SC_c in multilayered structures. $R_{SC/M}$ is the ratio of intensities of the SC to the main peaks on the XRSM, and "Amplitude" is the amplitude of the modulation wave generating the SC structure (Å). The periods of the multilayers were estimated by XRR measurements, and verified by a high-angle scan in θ-2θ using a kinematical model simulation.

	b	c	SC_b	SC_c	$R_{SC/M}$	Amplitude
Single Bi-2212	5.43	30.88	26.8	35.0	0.035	0.42
$(\text{Bi-2212}_4/\text{Bi-2201}_3)_6$	5.43	30.91	26.7	35.6	0.11	0.69
$(\text{Bi-2212}_2/\text{Bi-2201}_2)_6$	5.41	31.09	26.1	36.4	0.18	0.84

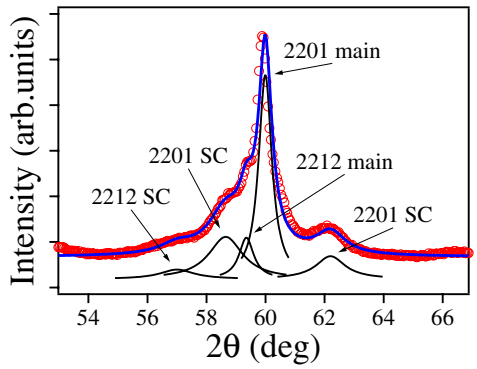

FIG. 4. (Color online) Projection of intensity to 2θ axis on the XRSM image. The intensity is fitted by five peaks: the main peaks of Bi-2201 and Bi-2212, the higher and lower SC peaks of Bi-2201, and the lower SC peaks of the Bi-2212 layers.

peaks. A cross section XRSM takes a slice image of $\omega \times 2\theta$ in reciprocal space, which can be rephrased on the Q_x-Q_y coordinate as

$$Q_x = \frac{2 \sin \theta}{\lambda} \sin(\omega - \theta), \quad Q_y = \frac{2 \sin \theta}{\lambda} \cos(\omega - \theta),$$

where λ is the x-ray wavelength (Cu $K\alpha_1$=1.5406 Å). Since these are rectangular coordinates, the modulation period can easily be estimated by the distance between the main and SC peak on the Q_x-Q_y coordinate. Table I shows lattice constants and modulation periods of each layer in the multilayered structure with a single Bi-2212 film as a reference.

The cross section XRSM revealed asymmetric SC peaks generated by the SC structure on a Bi-2212 film, which is described by a crystal model modulated by a sawtooth modulation wave.[11] In order to evaluate the amplitude of the modulation wave, the ratio of the main to SC peak ($R_{SC/M}$) simulated on the sawtooth model was compared to the experimental results. $R_{SC/M}$ was estimated by XRSM images simulated using DISCUS, a program for simulating crystal structures and calculating the corresponding reciprocal space.[13] $R_{SC/M}$ was experimentally obtained by peak fitting the projection of the intensity to the θ-2θ scan (Fig. 4). The $R_{SC/M}$ of Bi-2212 was ~0.1 in the multilayer instead of the ~0.04 found in the Bi-2212 film. On the sawtooth model

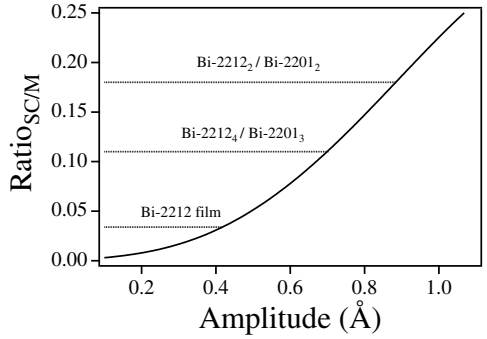

FIG. 5. Ratio of SC to main peak, $R_{SC/M}$, varied with the amplitude of the modulation wave, which generates the SC structure in Bi-2212.

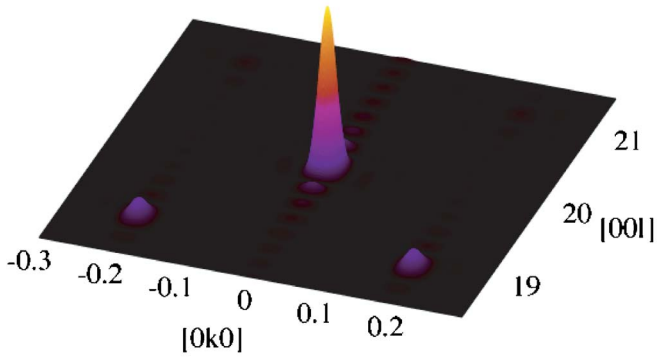

FIG. 6. (Color online) XRSM image simulated by sawtooth SC model with amplitude of 0.69 Å reveals asymmetric SC peaks around main peak of Bi-2212(00$\underline{2}$0). The peak ratio of $R_{SC/M}$ shows good agreement with experimental results on Bi-2212$_4$/Bi-2201$_3$.

with an amplitude of 0.4 Å, XRSM simulation showed $R_{SC/M}$=0.04. Repeated calculation with varied amplitude showed a correlation between amplitude and $R_{SC/M}$, as shown in Fig. 5. $R_{SC/M} \sim 0.1$ was obtained on the sawtooth model with an amplitude of 0.69 Å, as shown in Fig. 6. A modulation amplitude of 0.8 Å resulted in $R_{SC/M} \sim 0.2$, which was obtained experimentally on the multilayer structure of (Bi-2212$_2$/Bi-2201$_2$)$_6$.

Underdoped bismuth cuprate shows remarkable expansion of the modulation period[14,15] as opposed to the multilayered samples, which revealed almost the same period as the single film. Although multilayer strain affected the modulation period, the effect is negligible compared to the effect of extra oxygen; the effect of strain was more prominent on the modulation amplitude while the effect of extra oxygen played a dominant role on the modulation period. Taking aliovalent substitution as an example, the change in modulation period was not negligible; the effect of substitution must correspond with the effect of extra oxygen rather than lattice mismatch. Taking into account the slight expansion of the modulation period in the multilayer, oxygen atoms may transfer from the Bi-2212 layer to the underdoped intervening Bi-2201 layers. Bi-2201 film prepared by pulsed laser deposition method tends to show an underdoped nonsuperconducting phase.[16–19] A charge transfer[20] between Bi-2212 layer and the underdoped Bi-2201 layer might cause the T_c depression in the multilayered structure.

In summary, XRSM was performed on the multilayered bismuth cuprate high-T_c superconductor to investigate the dependence of the SC structure on multilayer strain, in which lattice mismatch was emphasized. Although the modulation period was slightly varied, the effect of strain was more prominent on the modulation amplitude while the effect of extra oxygen played a dominant role in the modulation period. We propose that oxygen content affects the size of the supercell (modulation period), while lattice mismatch dominates the arrangement in the supercell (modulation amplitude).

We wish to acknowledge K. Saito at Buruker AXS for support in the XRD measurements, and special thanks go to Y. Satoh at KITRI for maintaining the deposition system.

[1] Y. Matsui, H. Maeda, Y. Tanaka, and S. Horiuchi, Jpn. J. Appl. Phys., Part 2 **27**, L372 (1988).
[2] Y. Bando, T. Kijima, Y. Kitami, J. Tanaka, F. Izumi, and M. Yokoyama, Jpn. J. Appl. Phys., Part 2 **27**, L358 (1988).
[3] Y. Hirotsu, O. Tomioka, T. Ohkubo, N. Yamamoto, Y. Nakamura, S. Nagakura, T. Komatsu, and K. Matsushita, Jpn. J. Appl. Phys., Part 2 **27**, L1869 (1988).
[4] V. Petricek, Y. Gao, P. Lee, and P. Coppens, Phys. Rev. B **42**, 387 (1990).
[5] M. Zhiqiang, Z. Hongguang, T. Mingliang, T. Sun, X. Yang, W. Yu, and Z. Yuheng, Phys. Rev. B **48**, 16135 (1993).
[6] M. Zhiqiang, Z. Jian, T. Mingliang, X. Gaojie, X. Cunyi, W. Yu, Z. Jingsheng, and Z. Yuheng, Phys. Rev. B **53**, 12410 (1996).
[7] S. Kaneko, Y. Shimizu, and S. Ohya, Jpn. J. Appl. Phys., Part 1 **40**, 4870 (2001).
[8] E. E. Fullerton, I. K. Schuller, H. Vanderstraeten, and Y. Bruynseraede, Phys. Rev. B **45**, 9292 (1992).
[9] A. Vailionis, A. Brazdeikis, and A. S. Flodström, Phys. Rev. B **51**, 3097 (1995).
[10] S. Kaneko, K. Akiyama, Y. Shimizu, H. Yuasa, Y. Hirabayashi, S. Ohya, K. Saito, H. Funakubo, and M. Yoshimoto, J. Appl. Phys. **97**, 103904 (2005a).
[11] S. Kaneko, Y. Shimizu, K. Akiyama, T. Ito, M. Mitsuhashi, S. Ohya, K. Saito, H. Funakubo, and M. Yoshimoto, Appl. Phys. Lett. **85**, 2301 (2004).
[12] Z. Z. Li, H. Raffy, S. Bals, G. van Tendeloo, and S. Megtert, Phys. Rev. B **71**, 174503 (2005).
[13] T. Proffen and R. B. Neder, J. Appl. Crystallogr. **30**, 171 (1997).
[14] S. Kaneko, K. Akiyama, Y. Shimizu, Y. Hirabayashi, K. Saito, T. Kimura, H. Funakubo, M. Yoshimoto, and S. Ohya, Jpn. J. Appl. Phys., Part 1 **44**, 156 (2005).
[15] S. Kaneko, K. Akiyama, M. Mitsuhashi, Y. Hirabayashi, S. Ohya, K. Seo, H. Funakubo, A. Matsuda, and M. Yoshimoto, Europhys. Lett. **71**, 686 (2005).
[16] Y. Egami, H. Tabata, M. Kinugasa, T. Kawai, and S. Kawai, Jpn. J. Appl. Phys., Part 2 **30**, L478 (1991).
[17] K. Horiuchi, T. Kawai, M. Kanai, and S. Kawai, Jpn. J. Appl. Phys., Part 2 **30**, L1381 (1991).
[18] S. Zhu, D. H. Lowndes, B. C. Chakoumakos, J. D. Budai, D. K. Christen, X. Y. Zheng, E. Jones, and B. Warmack, Appl. Phys. Lett. **63**, 409 (1993).
[19] C. Marechal, R. M. Defourneau, I. Rosenman, J. Perriere, and C. Simon, Phys. Rev. B **57**, 13811 (1998).
[20] Z. Z. Li, H. Rifi, A. Vaurès, S. Megtert, and H. Raffy, Phys. Rev. Lett. **72**, 4033 (1994).